Optics Communications 422 (2018) 44–51

Contents lists available at ScienceDirect

Optics Communications

journal homepage: www.elsevier.com/locate/optcom

Improved multiphoton imaging in biological samples by using variable pulse compression and wavefront assessment

Martin Skorsetz, Pablo Artal, Juan M. Bueno *

Laboratorio de Óptica, Instituto Universitario de Investigación en Óptica y Nanofísica, Universidad de Murcia, Campus de Espinardo (Ed. 34), 30100 Murcia, Spain

ARTICLE INFO

Keywords:
Multiphoton microscopy
Pulse compression
Biological imaging

ABSTRACT

A variable prism-pair-based pulse compressor with wavefront aberration sensing was used to enhance multiphoton imaging in biomedical samples. This was incorporated into a custom-made microscope to reduce pulse temporal length, improve the quality of images of different layers of thick tissues and increase penetration depth. The laser beam aberrations were found to hardly change with the different experimental configurations of the pulse compressor. The optimum pulse compression state was maintained with depth within the tissue, independently of its thickness. This suggests that for each sample, a single experimental configuration is able to provide the best possible image at any depth location; although this needs to be experimentally obtained. Furthermore, a simple method based on laser average power reduction is presented to minimize the risk of photo-damage in biological samples. The use of pulse compression in multiphoton microscopy might have a potential for accurate and improved biomedical imaging.

1. Introduction

Over the last decades multiphoton (MP) microscopy has become a useful tool due to its inherent confocal properties, free-marker imaging conditions and minimized photo-damage effects [1]. Despite these optical sectioning capabilities, MP imaging at deeper layers within a sample is affected by aberrations and scattering that lead to blurred images with reduced contrast and resolution. Adaptive optics techniques have been used to improve MP imaging through the correction of the aberrations of the femtosecond (fs) laser beam, the microscope optics and the specimen itself [2–5]. However, these implementations only optimize the spatial properties of the beam to obtain a smaller focal spot.

Temporal properties of the illumination fs-laser are also of importance in MP imaging performance. Short pulses responsible for the generation of MP phenomena have a broad spectrum and they might suffer from chromatic dispersion due to the microscope optics and the sample itself. That is, the different frequency components travel at different speed and then the pulses are broadening in time. This limits MP efficiency and reduces imaging performance. To increase the effectiveness of MP processes, higher average laser power is needed. However, this increases the risk of non-controlled thermal side effects and photo-damage that should be avoided when imaging biological samples.

Pulse compression techniques are often used to restore "short laser pulses". Pulse compression devices use prisms [6], diffraction gratings [7] or chirped mirrors [8]. Most strategies are based on pre-compensation by measuring or estimating the temporal dispersion and apply the opposite so that the total dispersion is zero at the focal plane [9]. The implementation of pulse compression techniques into MP microscopy has been reported to increase imaging performance [10–13].

Müller and co-workers compared two-photon excitation fluorescence (TPEF) images of a fish retina using a double prism-pair dispersion pre-compensation unit [9]. They reported an increase in TPEF signal higher than 70% when comparing 170 and 340 fs laser pulses. A pulse compressor based on photonic crystal fibers was also combined with a MP microscope [13]. TPEF signal increased up to 7 times (in guinea pig intestine tissue and rat pulmonary artery cells) when using pulses of less than 35 fs (compared to 250 fs). A similar improvement (5.6× increase in TPEF) was reached with a grating-based pulse compressor when reducing the pulse duration from 190 to 38.7 fs [11]. With a two-prism pulse compressor used to reduce the pulse duration from 215 to 96 fs, second harmonic generation (SHG) signals from different collagen samples (liver, collagen gel, muscle) were improved 2×–3× [12]. Other authors reported up to 11-fold improvement in TPEF signal from cells and tissues, and up to 19-fold improvement in SHG images of a rat tendon specimen using sub-20 fs laser pulses [10].

* Corresponding author.
E-mail address: bueno@um.es (J.M. Bueno).

https://doi.org/10.1016/j.optcom.2017.12.040
Received 31 May 2017; Received in revised form 13 November 2017; Accepted 14 December 2017
Available online 8 January 2018
0030-4018/

An alternative approach to control chromatic dispersion includes pulse shapers. These are based on spatial light modulators and have also been reported to increase TPEF and SHG generation efficiency [14–16]. More recently a spatial light modulator and a deformable mirror have been combined with a MP microscope [17,18].

However, this previous literature on MP image improvement through pulse compression dealt with single plane imaging and results on thick samples are scarce [19,20]. An increase in TPEF imaging penetration in a labeled section of guinea pig detrusor was reported when using a grating-based pre-dispersion compensator [19]. TPEF and SHG signals from a human skin sample recorded with two compression states (120 and sub-20 fs) were compared [20]. Shorter pulses provided higher signal at different depth locations.

In the past, the limitations on MP imaging imposed by temporal pulse properties and the presence of aberrations (mainly from the sample) have been analyzed as independent issues. The usual adaptive optics MP microscopes only dealt with changes in aberrations [2–5]. On the other hand, improvements obtained after pulse compression did not have into account the effects of changes in the aberration pattern when modifying the optics of the compression device [9–13,19,20].

In this paper, we further analyze the effects of pulse compression on MP microscopy of biomedical samples. Thick samples from ocular tissues providing both TPEF and SHG signal were used in the experiment. We report on the use of a variable pulse compressor and a wavefront sensor introduced in the illumination pathway of the MP microscope. The temporal duration of the pulses is sequentially varied during MP imaging to obtain the optimum conditions for image improvement. The influence of the sample's depth location on the choice of the optimum compression conditions, and the corresponding improvement with depth are analyzed in detail. Moreover, the possible changes in the laser beam aberration are controlled through the wavefront sensor. If these are negligible, the spatial stability of the beam would allow isolating the effects of the pulse duration. Finally, the benefit of using pulse compression in order to reduced photo-damage is also discussed.

2. Methods

2.1. Experimental setup

The experimental setup combines a custom-built MP microscope and a two-prism-based pulse compressor (Fig. 1). The MP microscope is composed of a fs-laser source (760 nm), a XY scanning unit and an inverted microscope [5]. The pulse compressor (FemtoControl, APE, Berlin, Germany) was included in the illumination pathway and it was used to pre-compensate for the pulse dispersion induced by the microscope optics and the different imaged specimens. The different pulse compression states (PCSs) generated by the device were controlled through the user interface and depended on the prism positions and the used wavelength (see calibration procedure below). The non-linear signal (TPEF and/or SHG) emitted by the samples under study was detected through the same objective (in-air, long-working distance, 20×, $NA = 0.5$). This type of objective has been reported to be suitable for imaging ex-vivo ocular tissues and more recently to acquire SHG images from living human eyes (both cornea and sclera) [21]. A photomultiplier tube and a photon-counting unit were used in the registration pathway, together with TPEF/SHG spectral filters.

Additionally, the stability of the laser beam in terms of aberrations was also measured to analyze possible changes induced by the different PCSs due to the displacements of the prisms. For this, a Hartmann–Shack (HS) sensor was also placed in the experimental system as indicated in Fig. 1. From each HS image the wavefront aberration (WA) was calculated and expressed in Zernike polynomials up to 4th order for a diameter of 5 mm (see [22,23] for further details).

2.2. Image acquisition and samples

After the pulse compressor device was calibrated (see Results below), the different PCSs were used to improve the quality of the acquired MP images. The effectiveness of the pre-compensation technique was tested at randomly chosen planes within different samples and also for entire thick samples. For the former, a regular XY MP image was acquired for each PCS. The total intensity of each image was calculated and the PCS corresponding to the maximum value was chosen as the optimum PCS. To analyze the effect of sample's depth on the optimum PCS, a stack of images (for different depth locations) for the entire set of PCSs was recorded. It is interesting to notice that this action requires high acquisition times.

As biological specimens (not all shown here), different non-stained ocular tissues were imaged: a human epiretinal membrane, a rat retina, a piece of bovine sclera (fixed in paraformaldehyde), ex-vivo non-stained porcine, rabbit and chicken corneas, and a histological section of a rabbit cornea embedded in paraffin wax. Each sample has a different thickness, ranging between ~40 μm (epiretinal membrane and histological section) and ~500 μm (porcine cornea). Moreover, the specimen in paraffin presents reduced transparency. For a better discrimination, TPEF and SHG images are displayed in green and blue (false colors), respectively.

The use of tissue samples from animals and human donors in this study was approved by the Universidad de Murcia ethics committee and all procedures were carried out in accordance with the approved guidelines.

2.3. Calibration of the pulse compressor and laser pulse duration measurement

The pulse compressor was calibrated for the wavelength used in this work. Once the wavelength was introduced in the control panel, the positions of the prisms (in internal units) for the four basic settings were automatically set by the device. These were named as PCS0, PCS4, PCS8 and PCS12. A decrease in the prism position is associated with a reduction in the amount of prism glass introduced in optical pathway of the laser beam. Then, the prism positions corresponding to the basic PCSs were linearly interpolated to get 12 different PCSs. The next step was to measure the actual temporal duration of the laser pulses. An autocorrelator (Mini, APE, Berlin, Germany) was used for this. The pulse duration was measured at two different locations in the experimental system (see Fig. 1): at the exit of the pulse compressor (point A) with the configuration PCS0 (used as a reference) and at the entrance of the microscope (point B) for all PCSs from PCS0 to PCS12. This operation permits to investigate the temporal broadening of the pulse due to the optics, as well as to estimate the prism configuration providing the minimum pulse duration at the microscope entrance.

According to the manufacturer, the pulses emitted by the Ti–Sapphire laser (Mira 900f, Coherent) should have a pulse duration of 200 fs or less. The autocorrelator placed at the exit of the pulse compressor (point A in Fig. 1) set to PCS0 (i.e. no compression in operation) measured pulses of 230 fs (red dot in Fig. 2). As expected, due to the travel of the light beam through the optics of the experimental setup, the laser pulses at the microscope entrance (point B in Fig. 1) were broadened in time up to 400 fs (blue dot at PCS0 in Fig. 2). The PCS was then sequentially changed from PCS0 to PCS12 and, as shown in Fig. 2, a minimum in the pulse duration of ~150 fs was found for PCS7.

Since the minimum pulse duration shown in Fig. 2 might not lead to the best image at every depth location within the sample, we decided to use the term PCS throughout this paper. This might be due not only to the possible depth-dependent properties of the sample, but also to the non-negligible effects of the microscope objective. Although it is known that the PCS term is not a physical parameter, it will be used to facilitate the graphical representation of the results (i.e. the seeking

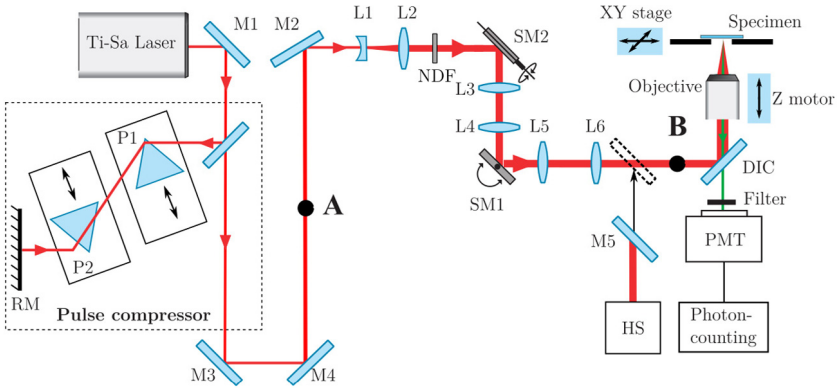

Fig. 1. Schematic diagram of the experimental setup. P1 and P2, prisms; M1–M5, mirrors; L1–L6, lenses; NDF, neutral density filter; SM1 and SM2, scanning mirrors; HS, Hartmann–Shack sensor; DIC, dichroic mirror; PMT, photo-multiplier tube.

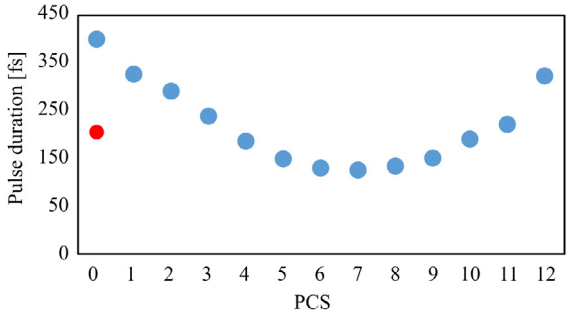

Fig. 2. Pulse compressor characterization. Pulse duration as a function of the PCS set in the device measured at the entrance of the microscope (location B, blue symbols). The red dot corresponds to the pulse duration measured at location A in Fig. 1. (For interpretation of the references to color in this figure legend, the reader is referred to the web version of this article.)

of the optimum PCS) and for a direct understanding of the experiment. For each example shown here, it is easy to check which is the actual duration of the pulse associated to the corresponding optimum PCS by only checking the data in Fig. 2.

3. Results

3.1. Wavefront aberrations vs. pulse compression

To evaluate if changes in the pulse compressor modified the spatial aberrations of the laser beam, HS images were recorded for each PCS. Some of the WA maps are depicted in Fig. 3a. A visual inspection reveals that the maps are similar. The averaged total RMS value was 0.213 ± 0.002 μm.

The contribution of the individual Zernike terms as a function of the PCS is presented in Fig. 3b (from 2nd to 4th order). The aberrations terms hardly change when modifying the PCS. Moreover, astigmatism Z_2^{-2} was found to be the dominant term.

For the sense of completeness, Fig. 4 shows both total (red symbols) and higher order (blue symbols) WA root-mean-square (RMS) values as a function of the PCSs. The effect of the compression on the measured pulse time is also depicted (gray symbols, values are the same as in Fig. 2). It can be observed that although the prisms are displaced to generate the different pulse temporal lengths, the laser beam aberrations kept stable.

3.2. Effects of pulse compression on a single plain

Fig. 5 shows the total intensity values for two different samples (providing TPEF and SHG signals) as a function of the PCS. The imaged plane within each specimen was randomly chosen.

For both samples the lowest intensity value was found for PCS0 (i.e. no pulse compression in operation). Furthermore, there was always a PCS providing a maximum intensity value. This optimum PCS depended on the imaged sample (PCS9 and PCS10 respectively). These results indicate that the pulse pre-compensation operation optimizes the efficiency of MP excitation processes while keeping the incident laser power constant. The improvements in signal ranged between 2× and 3×. The images corresponding to both PCS0 and the optimum PCS in Fig. 5 are presented in Fig. 6.

Fig. 7 illustrates the effectiveness of the pulse compression operation for both non-linear signals in the same specimen (histological sample of a rabbit cornea). The increase in signal was 2× and 1.8× for TPEF and SHG respectively. The corresponding images are also shown.

The intensity profiles along the horizontal line inserted in Fig. 7 are shown in Fig. 8. Since different parts of the cornea provide different non-linear signals, both SHG (stroma) and TPEF (keratocytes, epithelium and endothelium) intensity profiles are also plot together. This allows distinguishing the border between the different corneal structures what is important for some disease diagnosis in clinical environments.

It is interesting to notice that the optimum PCS does not correspond to the one providing the minimum temporal duration of the incident pulse (see Fig. 2). Since the pulse duration was measured at the entrance of the microscope (point B in Fig. 1), the effect of the objective can be the main reason. This fact suggests that this pre-compensation is then canceled by the objective (see Discussion for more details on this). Moreover, as the objective used was always the same, the small variations in the optimum PCSs can be attributed to the different nature of the specimens under study.

3.3. Effects of pulse compression on thick samples

The next step was to explore the benefit of pulse compression when imaging thick samples. For this, at each depth location within the sample a stack of MP images (one for each PCS) was acquired. Results are showed in Fig. 9 for an ex-vivo pig cornea.

This depicts the total intensity value of each SHG image as a function of both PCS and depth location (corneal layers located 30-μm apart). It can be observed that the optimum PCS does not depend on the depth, that is, there is only an optimum PCS which is the same for every depth location.

The reason for this is that the effects on pulse dispersion of the optics of the microscope are much higher than those of the sample itself. This result was the same for all the specimens involved in the experiment, but the optimum PCS differed among the samples. For instance, independently of the depth of the samples, PCS10 was the optimum PCS for a rabbit cornea and a human epiretinal membrane. However, the optimum state for a pig cornea was PCS8.

For a better understanding, Fig. 10 compares SHG images in a rabbit cornea without (PCS0) and with the optimum pulse compression

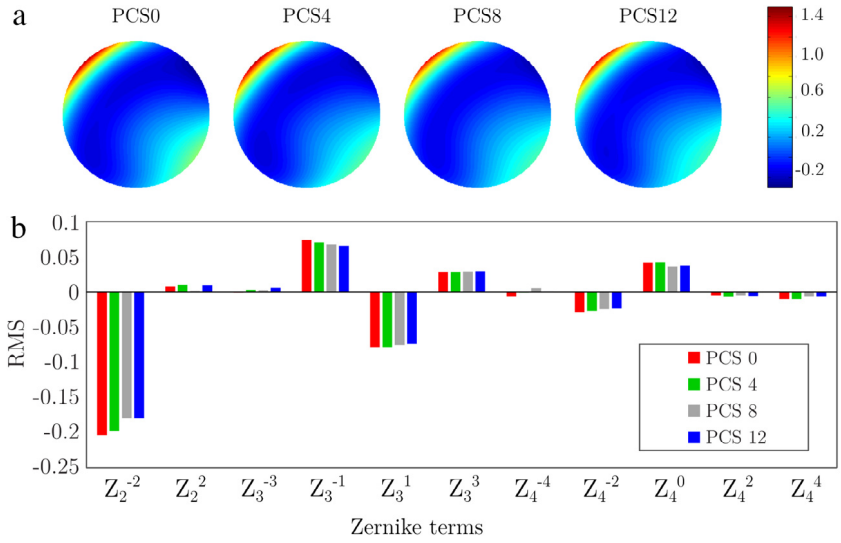

Fig. 3. (a) WAs corresponding to different PCSs. (b) Zernike coefficient values for different PCSs.

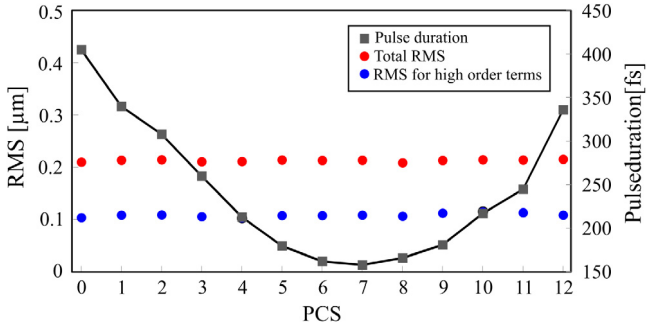

Fig. 4. Wavefront RMS values as a function of the PCS (red and blue dots). Gray symbols represent the pulse duration measured at the entrance of the microscope. Whereas the pulse duration is modified, the wavefront hardly changes. (For interpretation of the references to color in this figure legend, the reader is referred to the web version of this article.)

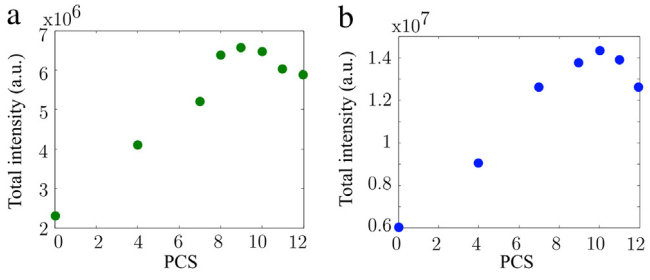

Fig. 5. Total TPEF (a) and SHG (b) intensity across the images as a function of the PCS for a single imaged plane in two samples: human epiretinal membrane (a) and ex-vivo porcine cornea (b).

(for this sample). Plots at the bottom are the associated histograms of intensity. These facilitate the understanding of the pulse compression effects in MP imaging. It can be observed that for every imaged plane the corresponding histogram moves to the right and spreads, what is representative of images with higher signal levels.

Fig. 11 depicts the averaged SHG intensity values for each depth location together with the corresponding plane-to-plane improvement (green symbols). This enhancement was fairly maintained with depth (averaged value: 1.62 ± 0.13).

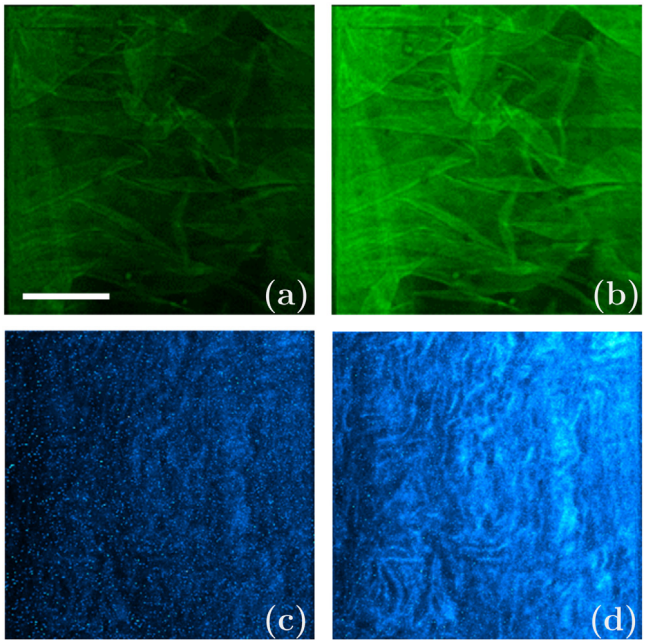

Fig. 6. Effects of pulse compression on TPEF (upper panels) and SHG (bottom panels) images. The improvements were respectively 2.25× and 2.38×. Bar length: 50 µm.

3.4. Reduced risk of photo-damage using pulse compression

It has been shown that pulse compression provides MP images with higher signal levels across the entire thick sample. Despite this image improvement, at deeper layers within the sample higher average laser power levels are sometimes required to get images with enough signal to correctly visualize some details and features. However, if this laser power is maintained constant, when imaging shallow layers non-controlled (and often non-reversible) photo-damage or photo-toxicity side effects might occur in the sample, what is a very important drawback in biological samples.

In this sense, a question still remains: how much can the laser average power be reduced when using pulse compression to get MP images with acceptable quality while avoiding possible photo-damage effects? To answer this question sets of images were recorded with the optimum

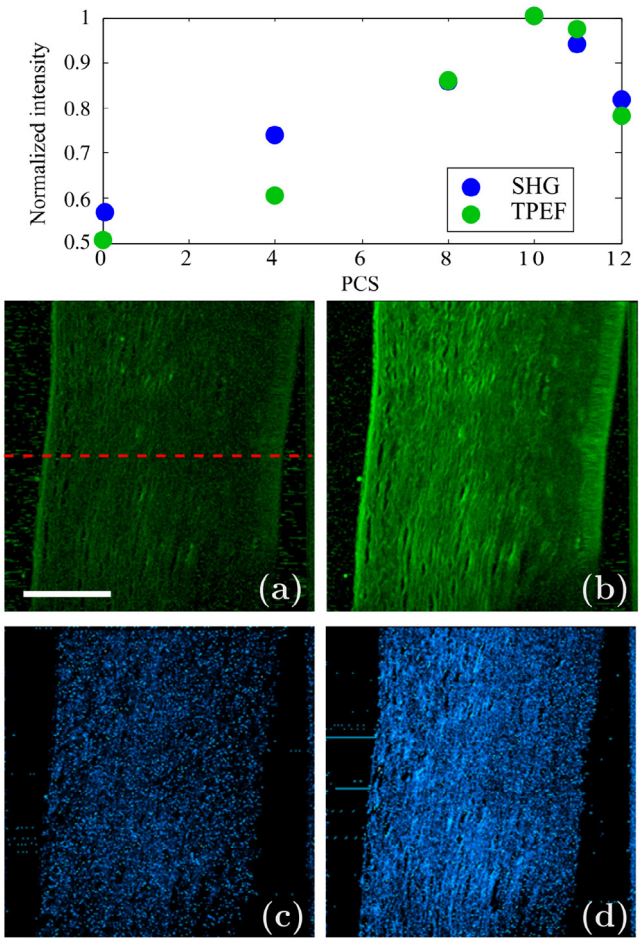

Fig. 7. Normalized total intensity for SHG and TPEF signals in the same sample as a function of the different PCSs (upper plot). For PCS8 and PCS10 green and blue symbols overlap. Images show the improvement in TPEF (middle panels) and SHG (bottom panels) for the same specimen. PCS0 (left) and optimum PCS (PCS10, right). Scale bar: 50 μm. Data along the horizontal dashed line are depicted in Fig. 8. (For interpretation of the references to color in this figure legend, the reader is referred to the web version of this article.)

PCS at different laser power levels and they were compared to the corresponding images acquired without pulse compression (i.e. PCS0).

The results corresponding to a sample providing TPEF signal (photoreceptor layer of a mouse retina) are depicted in Fig. 12. The upper plot depicts the square root of the TPEF intensity for images acquired without pulse compression (PCS0, red dot) and with the optimum PCS at different laser power values (blue dots). TPEF images (A, B, C and D) correspond to the labels in the plot. Image A corresponds to PCS0 and the pre-defined laser average power (red dot). When the optimum PCS was used, the TPEF signal effectiveness noticeably increased and image D was acquired. Then, with this optimum PCS in operation the laser power was progressively reduced (blue dots). This leads to a reduction in TPEF intensity. The acquired images B and C are representative of this. When qualitatively comparing images A and C, they look similar although the latter was acquired with less laser power. The histograms of these TPEF images are presented at the bottom plot for a quantitative comparison.

4. Discussion

Despite the intrinsic optical sectioning capabilities of MP microscopy, images are limited by spatial (aberrations, scattering) and temporal (optical dispersion) factors. The former is often corrected by means of adaptive optics procedures, which have been reported to enhance MP imaging [2–5]. On the other hand, optical dispersion produced by the refractive elements of the microscope and the sample itself broaden the temporal pulse length. The peak power is then reduced and also the effectiveness of the MP processes. As a consequence, higher laser power is needed to increase the generation of non-linear signal in order to get "better" images. For example, it has been reported that a 2-fold increase of pulse duration would require a power increase of 1.4-fold [24]. However, this might produce unwanted side effects on the sample (photo-damage, photo-toxicity) that should be avoided especially when imaging biological samples.

Here a research MP microscope has been modified to include a variable pulse compressor to manipulate and control the duration of the incident fs-laser pulses. The performance of the pulse compressor operation to improve MP images (especially at deeper locations within the sample) has been explored.

In this work, a pulse duration of 400 fs was reduced to 150 fs at the microscope entrance. This minimum pulse duration was obtained for PCS7. However, when imaging a sample the PCS providing this minimum pulse length does not correspond to the optimum PCS giving the best MP image. The fact that the optimum PCS at the microscope entrance occurs when the group velocity dispersion is over-compensated suggests this pre-compensation is canceled by the microscope objective. If so, the pulse duration might actually reach a minimum at the focus and this is the reason of having improved MP images.

Previous works used measurements of pulse duration at the focal point of the microscope objective [20]. However, it is well-known that pulse duration assessments of a non-parallel beam are not straightforward when using a commercially available auto-correlator (which usually requires a parallel beam). The present work overpasses this drawback since a unique microscope objective is used for the entire

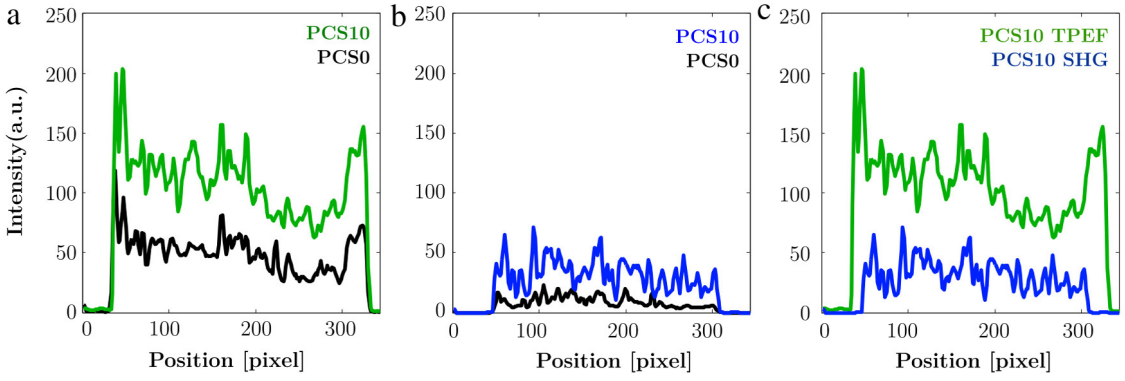

Fig. 8. Intensity values along the horizontal dashed line of Fig. 7. (a) TPEF signal without pulse compression (PCS0) and with the optimum compression (PCS10). (b) The same as in (a) but for SHG signal. (c) TPEF and SHG signals with the optimum PCS.

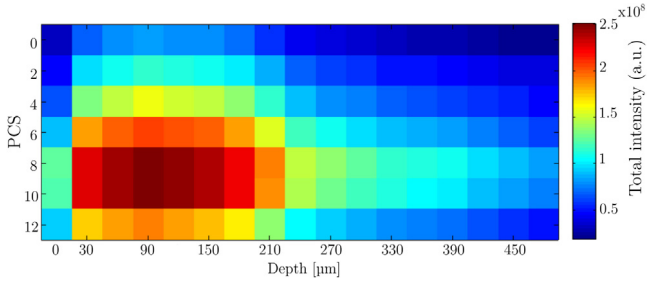

Fig. 9. SHG intensity map for different depth locations and PCSs in a thick porcine cornea sample.

experiment and the differences in the "optimal PCS" (measured at point B) are then exclusively due the samples themselves.

Moreover, our goal was neither to characterize the objective nor to determine the best pulse compression at the focal point, but to obtain the PCS configuration providing the best MP image (independently of the effects of the objective). In that sense, the procedure of sequentially changing the incident pulse width at the microscope entrance to explore the optimization of MP images was successfully proven here. To the best of our knowledge this procedure has not been reported in the literature previously.

Randomly chosen single planes of different samples were firstly improved (see Figs. 6 and 7). The optimum PCS (or alternatively the incident pulse duration) was particular for each sample and for all of them, a PCS higher that the #7 was necessary. With the optimum PCS, the acquired MP images presented higher intensity levels, with a better visualization of features. For samples providing both TPEF and SHG signals originated from the same plane the optimum PCS was shown to be the same (Fig. 7). This clearly differs from the results in [20] where the authors directly compared peak values (no images) originated at different layers only for two very different pulse laser conditions (sub-20 fs and 120 fs).

Total intensity improvements higher that 1.8× were found here. This enhancement in non-linear excitation efficiency is in agreement with studies found in the literature [9,12,19]. However, those previous studies did not look for the optimum pulse duration. Experiments therein were limited to compare MP images acquired without pulse compression and with the minimum pulse length reached with the compressor. As shown in the present work, this might underestimate the image improvement, what could be of importance at deeper locations within thick tissues (of special relevance if they present relatively low transparency).

Other experiments reported higher improvements (> 5×), but they managed with pulses below 50 fs [10,11,13]. These very short pulse durations could be more efficient to generate non-linear signals, but they are also more prone to have more non-controlled dispersion effects than conventional fs-laser pulses in the range 80–120 fs.

It is important to notice that the measured WA of the laser beam did not change with the different PCSs, what indicates that changes in MP image quality are exclusively driven by the effects of the pulse compression operation. To our knowledge, previous authors did not implement this laser beam WA assessment in pulse compression MP imaging. With the present experimental setup the WA was found to be stable. However, other devices based on diffraction gratings [7], chirped mirrors [8] or photonic crystal fibers [13] might not work similar and the WA could differ among the different pulse compression conditions, what might have a non-controlled impact on MP images.

Most of previous experiments combining pulse compression and MP imaging reported enhanced images for single planes. Although the impact of pulse compression on thick tissues is of great interest in biomedicine, only a few of studies were centered on those effects [19,20]. Here, a plane-by-plane searching of the pulse compressor

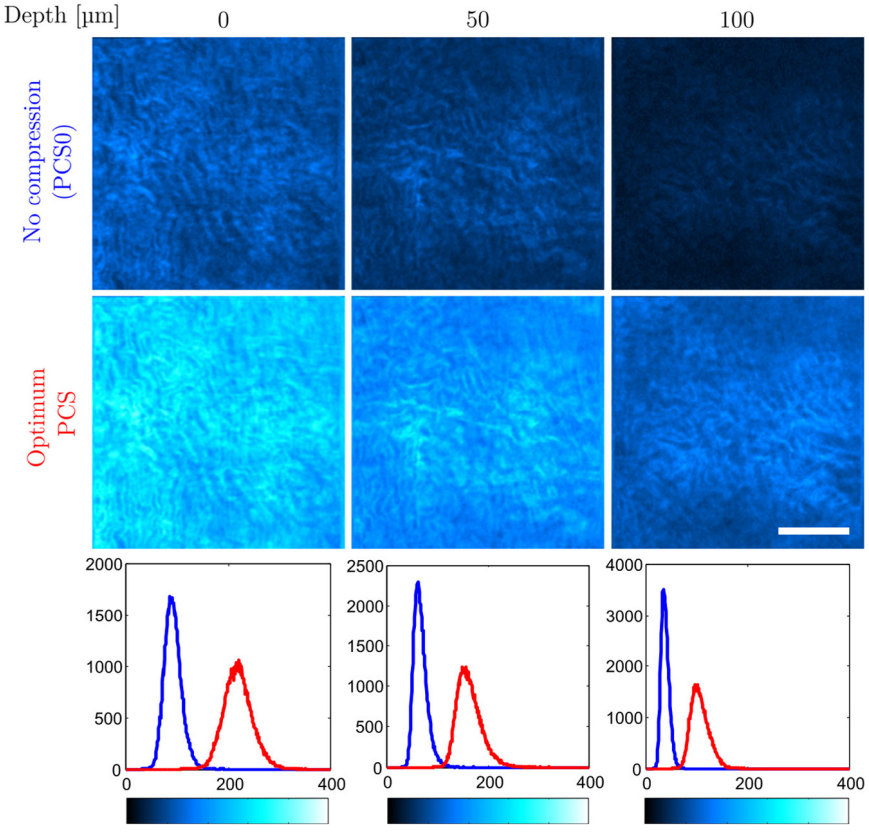

Fig. 10. Improvement of SHG images at different depth locations in a rabbit cornea using pulse compression. Associated histograms are presented at the bottom row (PCS0, blue; optimum PCS, red). Bar length: 50 µm. (For interpretation of the references to color in this figure legend, the reader is referred to the web version of this article.)

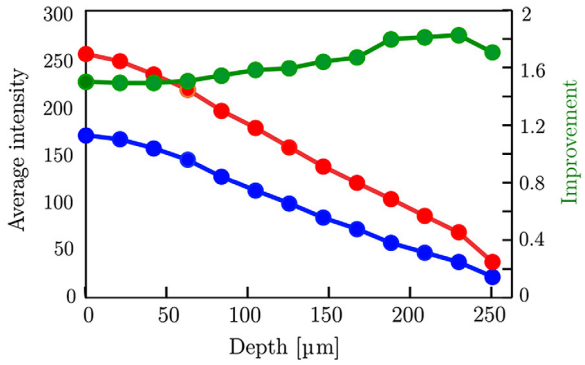

Fig. 11. Comparison of SHG intensity values before (blue) and after (red) pulse compression as a function of depth. Green data represent the corresponding plane-by-plane improvement. (For interpretation of the references to color in this figure legend, the reader is referred to the web version of this article.)

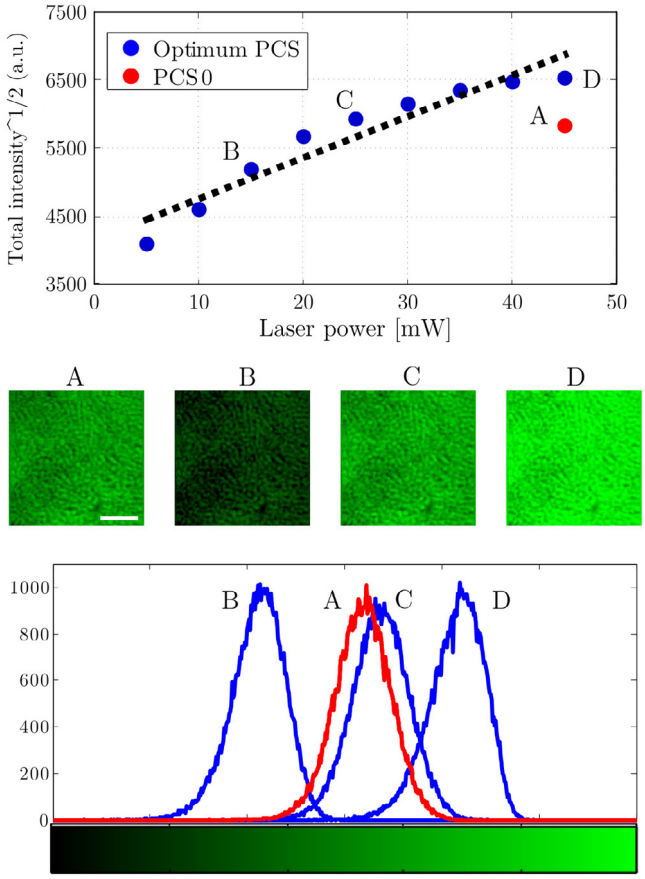

Fig. 12. Effects in TPEF signal when combining pulse compression effects and laser power reduction. Scale bar: 50 µm. Dashes line represents the best linear fit ($R^2 = 0.92, p < 0.0001$). See text for further details.

conditions giving the best MP image was also carried out. Results show that the optimum incident pulse length was the same for all the planes within the sample (Fig. 9). This means that the sample itself has little influence on pulse broadening and that most of these pulse broadening effects are due to the microscope optics.

Tang et al. also reported MP image enhancement at several depth locations, with a device providing a range of compression from ~400 to sub-20 fs [20]. They only presented the peak values of the MP images acquired with 120 and sub-20 fs laser pulses. The increase in the SHG intensity peak at 40 µm was of approximately 2.5×. Out from this location the improvement was lower. Moreover, they did not show MP images for direct comparisons.

Our experimental conditions did not allow us to go below ~150 fs. However, the procedure here developed was appropriate to get improved MP images, both SHG and TPEF. The enhancement at a certain depth location depended also on the used sample but it was never smaller than 1.5× for the samples here used. Moreover, when using the optimum pulse compressor conditions, the enhancement was shown to be fairly constant with depth.

It is also worth noticing that, due to the pulse compression operation in a thick sample, an increase in penetration depth appears (as seen in Figs. 10 and 11). This means that pulse compression is also able to improve images at deeper layers what is highly interesting due to the noticeable signal reduction at those locations. This penetration depth depends on the type of sample, and the choice of an ideal incident pulse length is crucial to maximize this effect. This fact was clearly shown in Fig. 9: If a non-optimum PCS is chosen, the penetration depth is clearly reduced.

This increase in MP imaging penetration here shown agrees with McConnell's results [19]. However, despite he used a labeled sample (stained guinea pig detrusor), the penetration improvement he reported was very limited (from 30 to 90 µm). Tang et al. used two different pulse lengths to compared TPEF and SHG peaks signals from a unique sample (human skin) at different depth locations. They claimed that sub-20 fs pulse provided images at a depth location 160% larger that those acquired with 120 fs [20]. Unlike Tang et al., in the present work it was not necessary to use very short pulses to obtain noticeable improvements. Moreover, the improvement was shown in a number of samples and the actual MP images were shown.

Finally, the benefit of using pulse compression to minimize damage in biological tissues has also been shown. With the pulse compression in operation, the incident laser average power was reduced until an image similar to that obtained without pulse compression was obtained. Results indicate that the laser power could be reduced up to 50% for both, TPEF and SHG signals. This is extremely important when imaging living specimens, where excessive exposure to light might put the sample under risk suffering irreversible photo-damage. Although out of the scope of this work, it is worth adding that photo-damage is not only associated with laser average power but also with instantaneous light intensity [25]. However, those effects are believed to be directly associated with living specimens rather than with ex-vivo biological samples as the ones here used.

Our results have been exclusively centered on pulse compression. However, specimens-induced aberrations (in particular spherical aberration) are also an important factor to be taken into account in MP imaging microscopy [2–5,26,27]. The detrimental effect might be important, what imposes a limit to the deeper plane within a sample that can be reached. Existing adaptive optics MP microscopes included a fixed in-cavity pre-compensation. Moreover, in those experiments the pulse length was neither measured nor optimized as we did here. To the best of our knowledge the combination variable pulse compression and WA sensing operation here shown has not been reported in the past. Since aberrations and chromatic dispersion are two independent physical phenomena, the combination of variable pulse compression and adaptive optics into a MP microscope might have a big potential for biomedical imaging.

5. Conclusions

A two-prism-based pulse compressor with aberration sensing has been shown to be a useful tool to increase the efficiency of MP processes and enhance the quality of both TPEF and SHG images. The use of an (experimentally computed) optimum incident pulse duration led to a significant improvement in the imaging independently on the thickness of the studied sample. Since a unique objective was used, the procedure here described does not require the assessment of the pulse length at

the focal plane of the objective. The pulse length was measured at the microscope entrance and this experimental condition providing the optimum PCS depended only on each sample. Images were sharper and brighter, presenting a marked enhancement and a better visualization of certain details. The benefits of this procedure as an alternative to reduce possible non-controlled photo-damage effects in biological samples have also been analyzed. This may even help to improve the performance of the ophthalmic MP-based imaging devices for clinical *in vivo* applications as very recently reported by these authors [21].

Acknowledgments

Supported by the Secretaría de Estado e Investigación, Desarrollo e Innovación (grant FIS2016-76163-R). Additional support was also provided by the European Research Council (Advanced Grant ERC-2013-AdG-339228 (SEECAT)) and the Fundación Séneca, Agencia de Ciencia y Tecnología de la Región de Murcia (grant 19897/GERM/15).

Disclosures

No conflicts of interest, financial or otherwise, are declared by the authors.

References

[1] F. Helmchen, W. Denk, Nat. Methods 2 (2005) 932.
[2] P.N. Marsh, D. Burns, J.M. Girkin, Opt. Express 11 (2003) 1123.
[3] M. Rueckel, J.A. Mack-Bucher, W. Denk, Proc. Natl. Acad. Sci. 103 (2006) 17137.
[4] D. Débarre, E.J. Botcherby, T. Watanabe, S. Srinivas, M.J. Booth, T. Wilson, Opt. Lett. 34 (2009) 2495.
[5] J.M. Bueno, E.J. Gualda, P. Artal, J. Biomed. Opt. 15 (2010) 66004.
[6] R.L. Fork, O.E. Martinez, J.P. Gordon, Opt. Lett. 9 (1984) 150.
[7] E. Treacy, IEEE J. Quantum Electron. 5 (1969) 454.
[8] R. Szipöcs, C. Spielmann, F. Krausz, K. Ferencz, Opt. Lett. 19 (1994) 201.
[9] M. Müller, J. Squier, R. Wolleschensky, U. Simon, G.J. Brakenhoff, J. Microsc. 191 (1998) 141.
[10] P. Xi, Y. Andegeko, D. Pestov, V.V. Lovozoy, M. Dantus, J. Biomed. Opt. 14 (2009) 14002.
[11] X. Liang, W. Hu, L. Fu, Opt. Express 18 (2010) 14893.
[12] A.M. Raja, S. Xu, W. Sun, J. Zhou, D.C.S. Tai, C.-S. Chen, J.C. Rajapakse, P.T.C. So, H. Yu, J. Biomed. Opt. 15 (2010) 56016.
[13] G. McConnell, E.G. Riis, J. Biomed. Opt. 9 (2004) 922.
[14] A.M. Weiner, Rev. Sci. Instrum. 71 (2000) 1929.
[15] B. Xu, Y. Coello, V. Lozovoy, M. Dantus, Appl. Opt. 49 (2010) 6348.
[16] J. Rehbinder, L. Brückner, A. Wipfler, T. Buckup, M. Motzkus, Opt. Express 22 (2014) 28790.
[17] B. Sun, P. Salter, M. Booth, Opt. Express 23 (2015) 19348.
[18] B. Sun, P. Salter, M. Booth, Opt. Lett. 40 (2015) 4999.
[19] G. McConnell, J. Biomed. Opt. 11 (2006) 054020.
[20] S. Tang, T.B. Krasieva, Z. Chen, G. Tempea, B.J. Tromberg, J. Biomed. Opt. 11 (2006) 020501.
[21] F.J. Ávila, J.M. Bueno, A. Gambín, P. Artal, Second harmonic generation microscopy of the human cornea and sclera in vivo, Invest. Ophthalmol. Vis. Sci. 58 (2017). ARVO E-Abstract 3109.
[22] J.M. Bueno, B. Vohnsen, L. Roso, P. Artal, Appl. Opt. 48 (2009) 770.
[23] E. Gualda, J.M. Bueno, P. Artal, J. Biomed. Opt. 15 (2010) 026007.
[24] W.R. Zipfel, R.M. Williams, W.W. Webb, Nat. Biotechnol. 21 (2003) 1369.
[25] A. Hopt, E. Neher, Biophysical J. 80 (2001) 2029.
[26] M.J. Booth, Light Sci. Appl. 3 (2014) e165.
[27] J.M. Bueno, M. Skorsetz, R. Palacios, E.J. Gualda, P. Artal, J. Biomed. Opt. 19 (2014) 011007.